

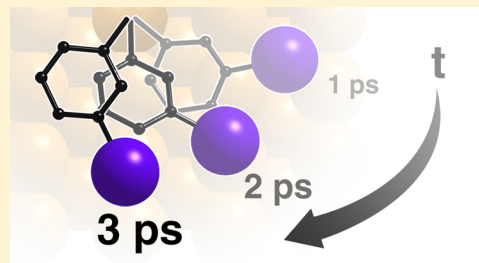
Clocking Surface Reaction by In-Plane Product Rotation

Kelvin Anggara,[†] Kai Huang,[†] Lydie Leung,[†] Avisek Chatterjee, Fang Cheng,[‡] and John C. Polanyi*

Lash Miller Chemical Laboratories, Department of Chemistry and Institute of Optical Sciences, University of Toronto, 80 Saint George Street, Toronto, Ontario M5S 3H6, Canada

S Supporting Information

ABSTRACT: Electron-induced reaction of physisorbed meta-diiodobenzene (mDIB) on Cu(110) at 4.6 K was studied by Scanning Tunneling Microscopy and molecular dynamics theory. Single-electron dissociation of the first C–I bond led to in-plane rotation of an iodophenyl (IPh) intermediate, whose motion could be treated as a “clock” of the reaction dynamics. Alternative reaction mechanisms, *successive* and *concerted*, were observed giving different product distributions. In the *successive* mechanism, two electrons successively broke single C–I bonds; the first C–I bond breaking yielded IPh that rotated directionally by three different angles, with the second C–I bond breaking giving chemisorbed I atoms (#2) at three preferred locations corresponding to the C–I bond alignments in the prior rotated IPh configurations. In the *concerted* mechanism a single electron broke two C–I bonds, giving two chemisorbed I atoms; significantly these were found at angles corresponding to the C–I bond direction for unrotated mDIB. Molecular dynamics accounted for the difference in reaction outcomes between the *successive* and the *concerted* mechanisms in terms of the time required for the IPh to rotate in-plane; in *successive* reaction the time delay between first and second C–I bond-breaking events allowed the IPh to rotate, whereas in *concerted* reaction the computed delay between excitation and reaction (~1 ps) was too short for molecular rotation before the second C–I bond broke. The dependence of the extent of motion at a surface on the delay between first and second bond breaking suggested a novel means to “clock” sub-picosecond dynamics by imaging the products arising from varying time delays between impacting pairs of electrons.



1. INTRODUCTION

A clock employs directional rotation of a hand as a measure of time. Similar rotary motion is required in the construction of molecular motors at surfaces.¹ The required motion has until now been induced by thermal energy² or by electrons^{3–6} delivered from the tip of a Scanning Tunneling Microscope (STM). These methods, however, give little directional preference. Here we use STM to show directional rotation in the product of surface reaction, and propose that this be used as a “clock” of the dynamics.

Surface reaction induced by electronic or photoelectronic excitation is topical in connection with the harnessing of solar energy. If the source of the impinging electron is an STM tip, pioneering studies have shown that the way is open to single-molecule chemistry.^{7–13} In light of the Ullmann reaction¹⁴ there has been long-standing interest in surface halogenation reactions, examined in many cases a molecule at a time.^{15–22}

The system studied here was the halogenation of copper by electron-induced reaction of meta-diiodobenzene (mDIB) on Cu(110) at 4.6 K. This molecule has been reported to react at elevated temperatures to form polyphenylene chains.^{20–22} At 4.6 K, however, it physisorbs intact, as in the case of other diiodobenzenes on this surface.^{23–27} In the present study, tunneling electrons delivered via the STM tip have been found to induce the breaking of the two C–I bonds in the molecule via electronic excitation. The reaction dynamics have been characterized by observing the recoil distance and direction of the products relative to the reagent.

In our earlier study of the reaction of para-diiodobenzene (pDIB),²³ the two C–I bonds reacted successively as a result of impact by two consecutive electrons. By contrast, for ortho-diiodobenzene (oDIB), the two C–I bonds were found to react in a concerted fashion following impact by a single electron.²⁴ In the present work we report that in the reaction of mDIB the two C–I bonds can react by both a *successive* and a *concerted* mechanism, these being major and minor alternative pathways. The products from each pathway were found to differ in terms of their angular distributions, being broad for the *successive* and narrow for the *concerted* mechanism. The broad product distribution observed in first C–I bond breaking in the *successive* mechanism was due to three different extents of in-plane directional rotation of meta-iodophenyl (IPh) radical. Modeling showed that the extent of IPh rotation correlated with the lifetime of the mobile IPh, increasing IPh lifetimes leading to increased rotation. Accordingly, the extent of in-plane rotation (at short, medium, or long times) constitutes a clock of the reaction dynamics. We propose a method to clock sub-picosecond reaction dynamics (without time-resolved STM) by introducing a variable delay, Δt , between pairs of electrons initiating first and second bond breaking; the first electron would release an intermediate (here IPh), and the second would remove it (by dissociating IPh here). The observed displacement of the intermediate (recoiling IPh in the

Received: March 24, 2016

Published: May 18, 2016



present case) would provide an experimental measure of its movement in the selected time interval, Δt .

2. RESULTS AND DISCUSSION

2.1. Physisorption. From the deposition of meta-diiodobenzene (mDIB) on Cu(110) at a maximum temperature of 12.6 K, we obtained the two physisorbed states shown in Figure S1. These two states differ in the alignments of their C_2 symmetry axis with respect to the underlying Cu row. By examining several large-scale ($500 \times 500 \text{ \AA}^2$) STM images, we found the major physisorbed state, “Row” ($56 \pm 5\%$), with its C_2 axis parallel to the Cu row, and the minor state, “Diagonal” ($44 \pm 5\%$), with its C_2 axis at an angle ($\sim 57^\circ$) to the Cu rows. Electron-induced reactions were examined for both physisorbed states, but are reported here only for the major state. The minor state, “Diagonal”, exhibited markedly different reaction dynamics and will be the subject of a succeeding paper.

As shown in Figure 1a, the physisorbed mDIB molecule (the major state) was imaged as a pair of bright lobes joined at one end, with an apparent height of $\sim 1.29 \text{ \AA}$. These two lobes were symmetrically placed on either side of the Cu row on which the mDIB molecule was physisorbed. The midpoint between these two lobes, indicated by the white cross (Figure 1a), was used to measure the distance traveled by the reaction products. Ab initio calculations were used to characterize the physisorbed state (see TH, Figure 1a). The adsorption geometry of mDIB was computed by initially assuming that the aromatic ring would lie flat on the surface, as found in studies of the physisorption of para- and ortho-diiodobenzene on metal surfaces.^{23,24} The most stable configuration ($E_{\text{ads}} = 1.04 \text{ eV}$) is shown in Figure 1a along with its calculated adsorption geometry and simulated STM image, which are in good agreement with the experiment. In the computed structure the molecule is physisorbed parallel to the surface plane with both I atoms located above Cu atoms and its aromatic ring centered near a short-bridge site, the two C–I bonds being located 61° to either side of the underlying Cu row as shown in Figure 1a. This (most stable) physisorbed geometry of mDIB on Cu(110) was previously reported in a density functional theory (DFT) study performed by Panosetti and Hofer.²⁸

2.2. Electron-Induced Reaction. Reaction of the physisorbed mDIB on Cu(110) was induced by the tunneling electrons from the STM tip, one molecule at a time. This procedure was as follows: (i) after imaging a single intact physisorbed mDIB molecule, the STM tip was placed over the center of the molecule (white cross in Figure 1); (ii) the tip height was adjusted; (iii) the feedback loop was deactivated, and a surface bias above +1.1 V was applied for up to 10 s. In step (iii), the tunneling current was recorded as a function of time, in which the reaction was identified by a single discontinuity in the current. Subsequent imaging of the same area confirmed that electron-induced reaction had occurred. Out of a total of 1069 dissociated physisorbed mDIB molecules, in the major pathway a single electron broke one C–I bond in 1040 cases ($97.3 \pm 3.0\%$) and, in the remaining 29 cases ($2.7 \pm 0.3\%$), broke both C–I bonds. A second electron was required in the major pathway to break the second C–I bond; this was examined in 90 cases. The two-bond breaking by two successive electrons is termed the “successive” pathway, whereas that in which a single electron breaks two C–I bonds is referred to as the “concerted” pathway. These two pathways are discussed in turn below.

MAJOR PATHWAY; SUCCESSIVE C-I

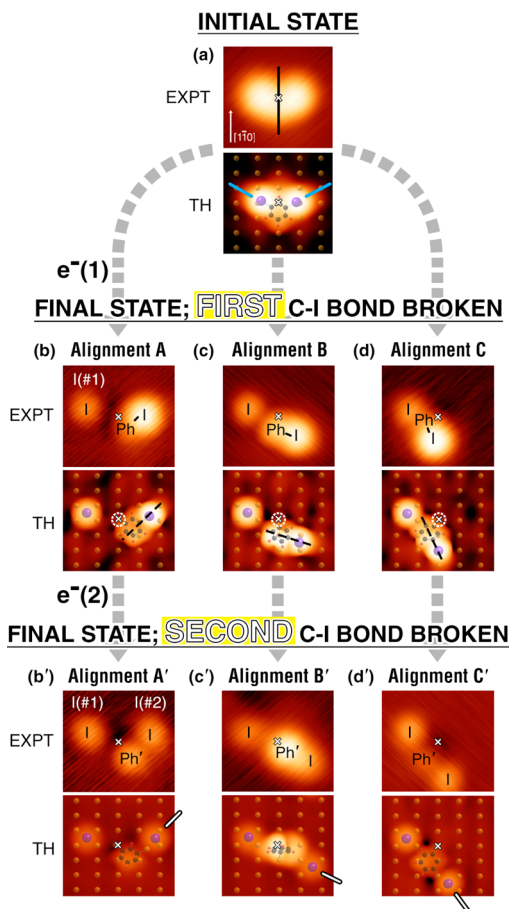


Figure 1. STM images (EXPT) and simulations (TH) from the major successive pathway of the electron-induced reaction of mDIB on Cu(110). Panel a shows initial state of physisorbed mDIB, with its C_2 symmetry axis (black line) and C–I bond directions (blue lines). The white cross marks the center of the intact mDIB reagent. Panels b, c, and d show the different characteristic product alignments (A, B, and C) after the first bond breaking, each alignment consisting of I atom(#1) and IPh. Alignments A, B, and C differ by the extent of IPh in-plane rotation. The black dashed lines indicate the computed C–I bond direction in IPh. In panels b, c, and d, the Cu atoms atop which the IPh radical chemisorbed are circled by a white dashed circle. Panels b', c', and d' show the three product alignments (A', B', C') following the subsequent second bond breaking, which consists of I atom(#2) and Ph'. The white line indicates the recoil direction of I atom(#2) which correlates with the C–I bond direction in its parent IPh. STM images ($2 \times 2 \text{ nm}^2$) were taken at 4.6 K in constant-current mode with a sample bias of +0.1 V and a current set point of 0.2 nA.

2.2.1. Successive Pathway. In the case of the successive pathway, we present the three product alignments consisting of an I atom(#1) and meta-iodophenyl (IPh) in Figure 1 with their corresponding computed and simulated geometry. The probability of each product alignment (see panels b, c, and d) was 276 cases for alignment A ($26.5 \pm 1.6\%$), 296 for alignment B ($28.5 \pm 1.7\%$), and 400 for alignment C ($38.5 \pm 1.9\%$). As shown in Figures 1b–d, the IPh product was imaged as a bright oval, found experimentally at three different alignments in the surface plane, in agreement with the C–I bond directions in the theoretical simulations (TH) from three computed geometries. The IPh chemisorbed atop the same Cu atom underneath the prior mDIB reagent (white dashed circle,

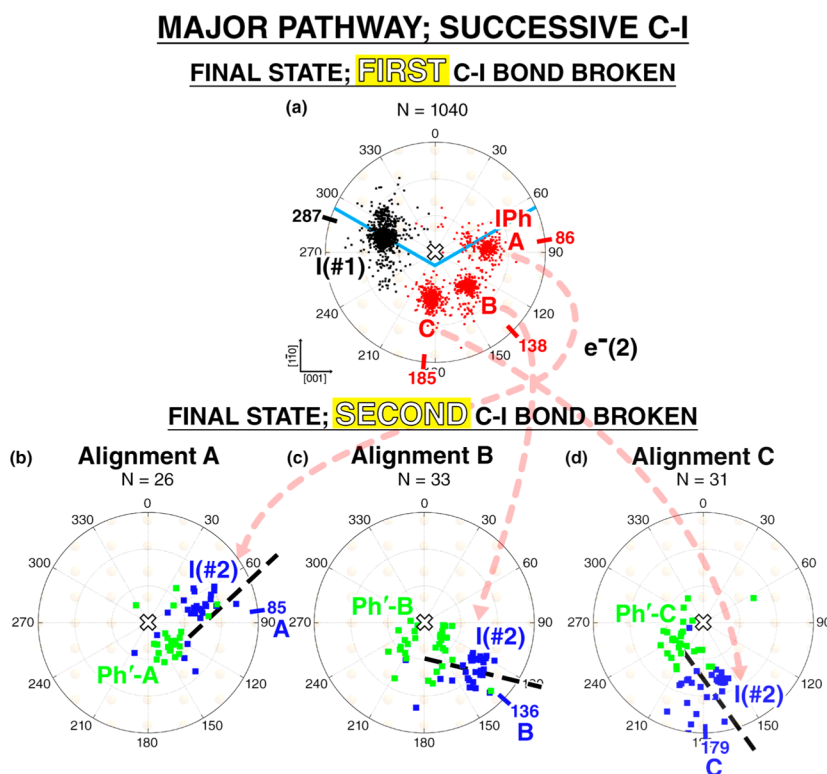


Figure 2. Distance and angle distributions of products in the *successive* reaction pathway for first and second bond breaking. Panel a shows the final positions of I atom(#1) (black squares) and IPh (red squares) from the first bond breaking. The blue lines in panel a indicate the computed C–I bond directions in the intact mDIB. Panel b shows the final positions of I atom(#2) (blue squares) and Ph' (green squares) from second bond breaking in alignment A. Panels c and d show the same as in panel b but for alignments B and C. The black dashed lines indicate the computed C–I bond directions of the parent IPh reagent in each pathway. The origin of the polar plot is indicated by a white cross, which marks the center of the intact mDIB; the distance between the concentric circles in the plot is 3.61 Å. All angles were measured from the $[1\bar{1}0]$ direction in the clockwise direction. The colored ticks on the circular axis of the plots indicate the average angle at which the products were scattered.

Figures 1b–d). These three alignments accounted for $93.5 \pm 3.0\%$ of the 1040 physisorbed mDIB molecules dissociated. In the remaining small number of cases (68 cases; $6.5 \pm 0.8\%$), we observed a variant binding of the IPh radicals in which the IPh was displaced laterally by 1–2 lattice constants along $[1\bar{1}0]$, away from the Cu atom underneath the prior mDIB reagent.

The polar plot of Figure 2a shows the angular and distance distribution of the reaction products from the first bond-breaking events of the *successive* pathway. The data were reflected so that I atom(#1) was located at the left of the polar plot. The three alignments of the IPh radical correspond to three locations of the bright spot in the STM image, indicated as A, B, and C in Figure 2a. The bright spot in the STM image of IPh corresponds to the I atom within the IPh radical, as obtained from the theoretical simulation. The I atom of the intact IPh in alignments A, B, and C were located in three directions away from $[1\bar{1}0]$ at 86° , 138° , and 185° ($\pm 5^\circ$) (the trimodal distribution is clearly evident in the three peaks in the histogram of Figure S2). This shows that IPh rotated in-plane to three different angles, as its I atom was displaced to three locations on the surface. The chemisorbed I atom(#1) released in the first bond breaking was located on average 5.4 ± 0.8 Å from the center of the intact molecule, at $73 \pm 14^\circ$ from the $[1\bar{1}0]$ direction (shown as 287° in Figure 2a). It was scattered along the computed C–I bond (#1) direction of the intact molecule at 61° to $[1\bar{1}0]$, consistent with the I atom(#1) having recoiled along its prior bond direction as observed in earlier work.²⁶

In electron-induced reaction at surfaces reagents are subjected to an impulse for femtoseconds while in the anionic state.^{29,30} Subsequently for picoseconds they traverse the ground potential-energy surface (pes), consequently it is of interest to examine the ground pes. Ab initio calculations showed that the reaction of mDIB across this surface was exothermic, producing I atom(#1) and IPh. The exothermicities were computed as 1.00 eV to form I atom(#1) plus IPh-A, 1.22 eV to form I atom(#1) plus IPh-B, and 1.24 eV to form I atom(#1) plus IPh-C. This substantial energy release is consistent with the computed low energy barrier for C–I bond breaking of 0.20 eV for all three outcomes (computed by a climbing image nudged elastic band (NEB) technique).³¹ The three differently aligned IPh radicals were found to be stable chemisorbed states bound to the same Cu atom reached by in-plane rotation across energy barriers of ~ 0.1 eV. The C–I bond direction of the chemisorbed IPh relative to the $[1\bar{1}0]$ direction was computed to be 56° for alignment A, 114° for alignment B, and 153° for alignment C. By comparing these angles with the initial C–I bond direction in the mDIB reagent (61°), IPh-A has rotated anticlockwise by the small amount of 5° , IPh-B and IPh-C clockwise by 53° and 92° .

The angular alignment of the IPh was confirmed by inducing the dissociation of the second C–I bond in the chemisorbed IPh radicals with a second electron. Voltage pulses above a threshold of approximately +1.6 V were required to dissociate each of the three IPh—A, B and C—yielding an I atom(#2) and a meta-phenylene radical (Ph') at the surface as shown in Figures 1b'–d'. The angle and distance distributions of the

second bond-breaking event are presented in Figures 2b–d. The I atom(#2) recoiling from IPh in alignment A, B, or C is seen to chemisorb at three different 4-fold hollow sites, located at $85 \pm 34^\circ$, $136 \pm 19^\circ$, and $179 \pm 19^\circ$ from the $[1\bar{1}0]$ direction (see also histogram in Figure S2), which are similar to their locations in the IPh, as noted in Figure 2a. These recoil angles correspond to the alignments of the C–I bond in the intact IPh from which I atom(#2) came, as indicated by the black dashed line in Figures 2b–d (these angles were 56° for alignment A, 114° for alignment B, and 153° for alignment C with respect to $[1\bar{1}0]$). The correspondence between the three C–I bond directions in the intact IPh in alignments A, B, and C and the three recoil directions for I atoms(#2) coming from second bond breaking in alignments A', B', and C' provides independent confirmation of the existence of three differently rotated configurations of IPh.

Figure 3 shows the three stable configurations observed for phenylene, Ph', following second C–I bond breaking in the successive reaction. In more than half of the cases (~65%) I atom(#2) was accompanied by stable Ph' in one of three configurations distinguished by measured height, as shown in

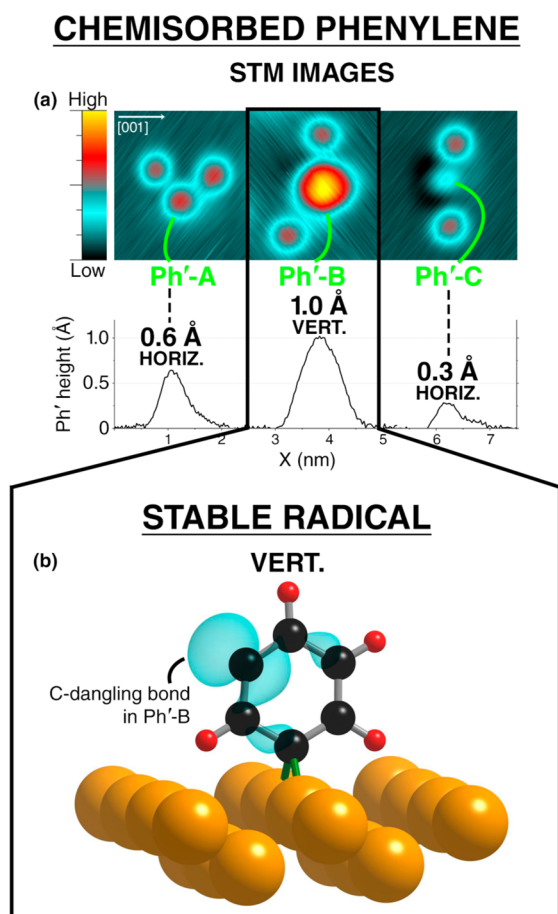


Figure 3. Panel a gives STM images of three different Ph' configurations, obtained from electron-induced reactions of mDIB on Cu(110). STM images ($2 \times 2 \text{ nm}^2$) were taken with a sample bias of +0.1 V and a current set point of 0.2 nA. Panel a also gives three corresponding height profiles measured along $[001]$. Panel b gives the spin density ($\rho = \rho_{\text{spin-up}} - \rho_{\text{spin-down}}$, isocontour = $0.0005 \text{ e}^-/\text{\AA}^3$) of vertical Ph'-B in its ground electronic state (with a computed magnetic moment of $\sim 1 \mu_B$), showing the existence of a C dangling bond pointing away from the surface. Only positive charge density is shown.

Figure 3a: IPh-A gave Ph'-A of $\sim 0.55 \text{ \AA}$ height, IPh-B gave Ph'-B of $\sim 0.97 \text{ \AA}$ height, and IPh-C gave Ph'-C of $\sim 0.32 \text{ \AA}$ height. The tall Ph' of Ph'-B is thought to be a chemisorbed phenylene with a vertical ring, since its height matches that reported for vertical phenyl on this surface.^{11,32} This structure, Ph'-B, should therefore have a carbon dangling bond pointing away from the surface, as pictured in Figure 3b.

2.2.2. *Concerted Pathway.* Figure 4 gives the initial and final state images obtained in 29 cases of the minor reaction pathway for electron-induced reaction of mDIB, designated as *concerted* in which one electron (see below) breaks two C–I bonds. The appearance of the physisorbed reagent molecule in the 29 cases of this concerted bond breaking was indistinguish-

MINOR PATHWAY; CONCERTED C-I

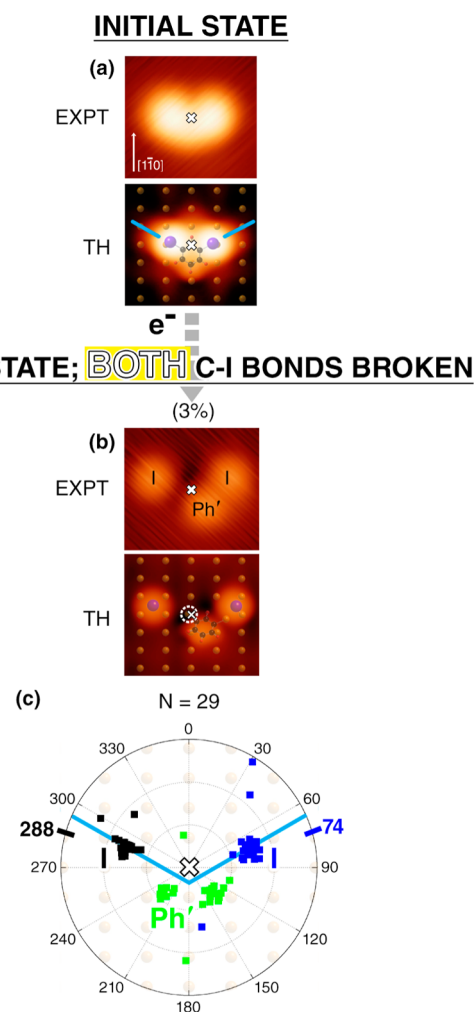


Figure 4. STM images (EXPT) and simulations (TH) from the concerted pathway in which two C–I bonds of mDIB were broken, giving two I atoms and a Ph'. Panels a and b show the initial and final states of the reaction. The white cross marks the center of the mDIB reagent. The initial C–I bond directions in mDIB are given as blue lines. STM images ($2 \times 2 \text{ nm}^2$) were taken with a sample bias of +0.1 V and a current set point of 0.2 nA. Panel c shows the distance and angular distribution of the products as a polar plot. The I atoms recoil along the reagent C–I bond directions, without rotation. The average scattering directions are indicated by colored ticks on the circular axis of the plot. All angles were measured from the $[1\bar{1}0]$ direction in the clockwise direction. The distance between the concentric circles in the polar plot is 3.61 \AA .

able from that which yielded the major *successive* reaction pathway. The data were collected at the bias of +1.40 V. We shall show (section 2.4) that we can account for the existence of this minor pathway if we assume that there is the possibility of formation of an anionic state with marginally ($\sim 2\%$) longer lifetime than characterizes the major pathway. We note that the term “concerted” does not imply simultaneous bond breaking.

Figures 4a,b show a representative case of the *concerted* pathway, in which a physisorbed mDIB molecule was dissociated to yield two I atoms and a Ph' at the surface. In contrast to the *successive* reaction pathway the *concerted* pathway gave a single pattern of I atom reaction products with the two atoms scattered symmetrically at $\pm 73^\circ$ away from the $[1\bar{1}0]$ axis (shown as 288° and 74° in Figure 4c). Significantly, the two I atoms have recoiled along the C–I bond directions in the unrotated physisorbed reagent, mDIB. Each I atom was chemisorbed to the nearest 4-fold hollow sites along the prior C–I bonds. The Ph' fragment was found to be doubly bound to the surface, one of its C atoms bound to the Cu atom beneath the reagent molecule, and the other to an adjacent Cu atom as shown in Figure 4b. The single alignment of Ph' obtained from the *concerted* pathway was identical to that from alignment A' in the *successive* pathway (Figure 1b'). The outcome of *concerted* reaction clearly resembles that expected for unrotated mDIB.

2.3. Reaction Mechanism. We have measured the average single-molecule reaction rate as a function of the STM current, in order to determine the number of electrons responsible for the individual reactive events. This method was introduced by Ho,¹⁰ and recently detailed by Riedel.³³ We have modified the method to include the case of competing pathways (see section 3 in Supporting Information). As shown in Figure 5a, it was found that the reaction rates in both pathways, first C–I bond breaking in *successive* reaction and both C–I bonds in *concerted*, scaled linearly with the current at a tunneling bias of +1.40 V, indicative of a one-electron process. On the basis of this linear dependence of reaction rate on current, we can discount the effect of the electric field as the cause of reaction.

The relatively high voltage of +1.1 V required to induce reaction indicates the involvement of the electronic excitation in both reaction pathways. Electrons of comparable energy were shown in earlier work of this laboratory^{24,34} to break the C–I bonds of pDIB and oDIB physisorbed on the same surface. In the present case the computed projected densities-of-states (pDOS), shown in Figure 5b, revealed that the lowest unoccupied molecular orbital (LUMO) exhibited a nodal plane between carbon and iodine atoms, evidence of a σ^* antibonding character with respect to the C–I bond. The LUMO was computed to be ~ 0.9 eV above the Fermi level. The measured yields for electrons of ~ 1.4 eV were $\sim 10^{-10}$ reactive events/electron for the first C–I bond in the *successive* pathway, and $\sim 10^{-12}$ reactive events/electron for the *concerted* pathway. Vibrational excitation was unlikely, given that the vibrational energy was computed to be < 400 meV for the stiffest C–H stretching mode in mDIB physisorbed on Cu(110).

2.4. Dynamics. Theoretical modeling using DFT-based molecular dynamics trajectory calculations was employed to obtain the dynamics in both the *successive* and *concerted* pathways. The “Impulsive Two-State” (I2S) model developed in earlier work of this laboratory^{23–26} embodies an empirical anionic potential-energy surface (pes*), and an ab initio neutral ground-state potential-energy surface (pes). Given that the

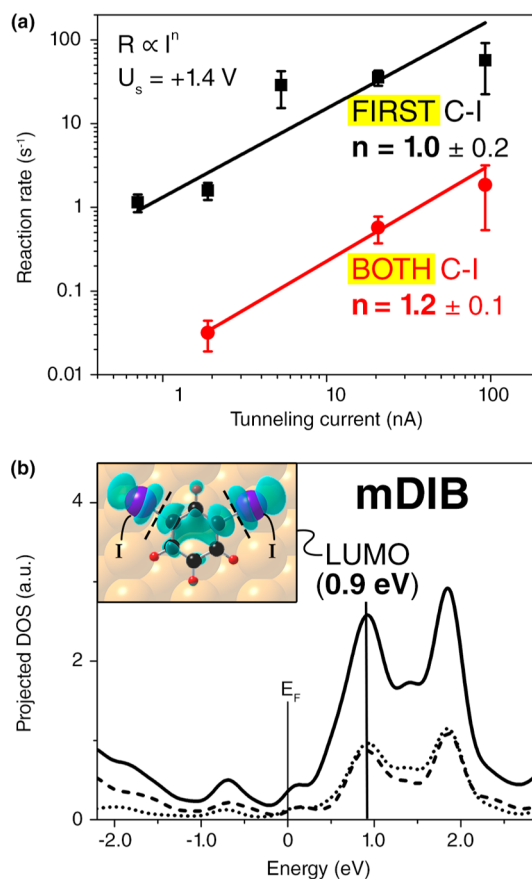


Figure 5. Panel a shows, in a log–log scale, the reaction rate as a function of tunneling current for the first C–I bond breaking process of the *successive* pathway (in black), and the breaking of both C–I bonds in the *concerted* pathway (in red). The reaction rates were measured at a tunneling bias of +1.4 V. A linear fit gave a slope of $n = 1.0 \pm 0.2$ for the *successive* pathway, and a slope of $n = 1.2 \pm 0.1$ for the *concerted* pathway. Panel b shows that the lowest unoccupied molecular orbital (LUMO) is aligned 0.9 eV above Fermi level, as in the projected density-of-states (pDOS) of intact mDIB reagent. The solid, dashed, and dotted lines show the pDOS of the adsorbate, its I atom, and the C atom beside the I atom, respectively. The inset in panel b visualizes the electron density of the LUMO of mDIB in real space (isocontour = $0.0005 \text{ e}^-/\text{\AA}^3$); the dashed black lines show the nodal planes between the C and I atoms, indicative of a C–I σ^* antibonding character.

reaction was induced by electron tunneling to the C–I antibonding orbital, this pes* was constructed by placing extra electron charge in the I atoms of the molecule, which gave C–I repulsion that triggered reaction. To generate an ionic pseudopotential for I⁻, we used the configuration $[\text{Kr}]-4d^9 5s^2 5p^6$. This approach has been shown in our earlier work to give an informative description of electron-induced reaction at metal^{23–26} and semiconductor³⁵ surfaces (see **Materials and Methods in Supporting Information**).

2.4.1. Successive Pathway. We simulated the anionic potential surface by partitioning a full electron charge between the two I atoms of the physisorbed mDIB. The procedure was identical to that employed in our earlier work on pDIB and oDIB on the same Cu(110) surface.^{23–26} The system was excited from the stable physisorbed ground state to the empirical anionic potential to evolve for a residence time of t^* , gaining momentum in the anionic state. It was then returned with its accumulated momentum to the ground potential to

evolve for up to 3.4 ps. The partitioning of the electron charge was the input parameter selected to give the observed outcome.

Figure 6 gives trajectories that reproduce the observed three product alignments in the *successive* pathway. Product alignment

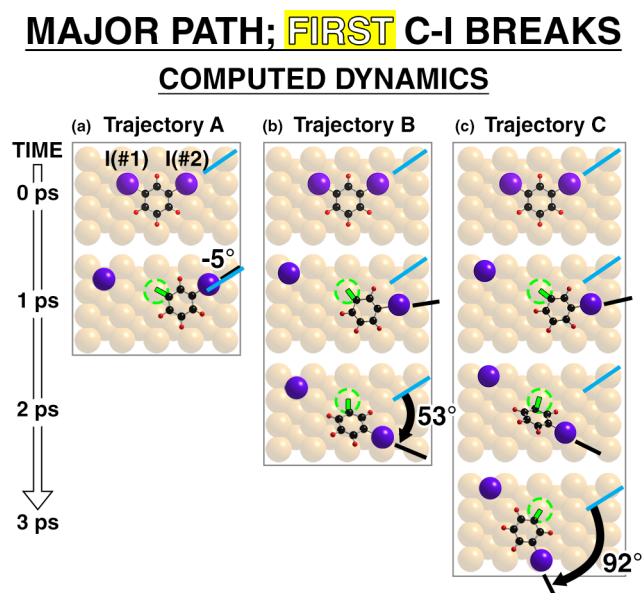


Figure 6. Computed dynamics for *successive* pathway. Panels a, b, and c show the time evolution of the systems in giving product alignments A, B, and C. To obtain alignment A, a half-electron was placed in I(#1) and in I(#2) for $t^* = 56$ fs. To obtain alignment B, $0.8 e^-$ was placed in I(#1) and $0.2 e^-$ was placed in I(#2) for $t^* = 42$ fs (t^* is in trajectories A and B the minimum value to give reaction). To obtain alignment C, one electron was placed in I(#1) for $t^* = 36.5$ fs. The green lines in all panels show the C–Cu bond toward the Cu atom indicated by the green dashed circles. The blue line indicates the initial C–I bond direction of the IPh, while the black line indicates the instantaneous C–I bond direction of the IPh at the indicated time following electron attachment.

A was obtained when an extra electron was placed equally on I atoms(#1) and (#2), for minimum residence time of $t^* = 56$ fs in the anionic state; alignment B was obtained by placing an unequal charge distribution of $0.8 e^-$ and $0.2 e^-$ for I atoms(#1) and (#2), for minimum residence time of $t^* = 42$ fs, and alignment C by placing the extra electron only on one I atom (I atom(#1) of Figure 6c), for residence time of $t^* = 36.5$ fs in the anionic state (the minimum residence time of 36 fs gave IPh in alignment C, but the I atom displaced by 2.5 \AA from the observed mean position, along $[1\bar{1}0]$). The values of t^* employed were found in the femtosecond range, characteristic of the anion lifetimes at a metal surface.³⁶

Computationally, after the system returned to the ground state, for all three cases, the C–I bond (#1) broke and propelled I atom(#1) along its prior bond direction, in agreement with experiment. The dangling bond in IPh formed after the C–I bond broke and experienced attraction to form a C–Cu bond, which caused the in-plane rotation of the IPh. Notably the attractive force acts as a torque that imparts a clockwise angular momentum (see Figure 6) to the IPh, whose center of mass is on the heavy I atom. The rotation took place on a picosecond time scale as follows: in trajectory A the IPh rotated to its final alignment within 1 ps; in trajectory B the IPh rotated through the potential well of IPh-A before reaching its final alignment B, in about 2 ps; in trajectory C the IPh rotated

through the potential wells of IPh-A and IPh-B before reaching its final alignment C in about 3 ps.

2.4.2. Concerted Pathway. Extensive trajectory calculations by the I2S model revealed that the *concerted* outcome could not be achieved by partitioning a single electron over the two I atoms using the minimum t^* . Since the *concerted* reaction resembled path A of *successive* reaction, we adopted the equal ($0.5 e^-$, $0.5 e^-$) charge distribution that led to alignment A and examined the effect of a minimal increase in the lifetime of the anionic state. Increase in t^* from 56 to 57 fs was found to alter the dynamics from *successive* reaction to *concerted*. This suggests that the minor pathway (3% of the total reaction) may be due to a small minority of anions that live for an additional ~ 1 fs. The observed low yield of *concerted* reaction may therefore be linked to the anticipated steep decrease in ionic survival probability at a metal surface with time.³⁷

As outlined in Figure 7a the above I2S model of *concerted* reaction is one in which the first C–I bond breaks promptly, leaving internally excited IPh that proceeds to break its second C–I bond after ~ 1.2 ps (the time of C–I (#2) bond breaking is shown as 1.2 ps in Figure 7b). Both I atoms recoil along the initial C–I bond directions, as observed experimentally, since

MINOR PATH; BOTH C-I BREAK
COMPUTED DYNAMICS

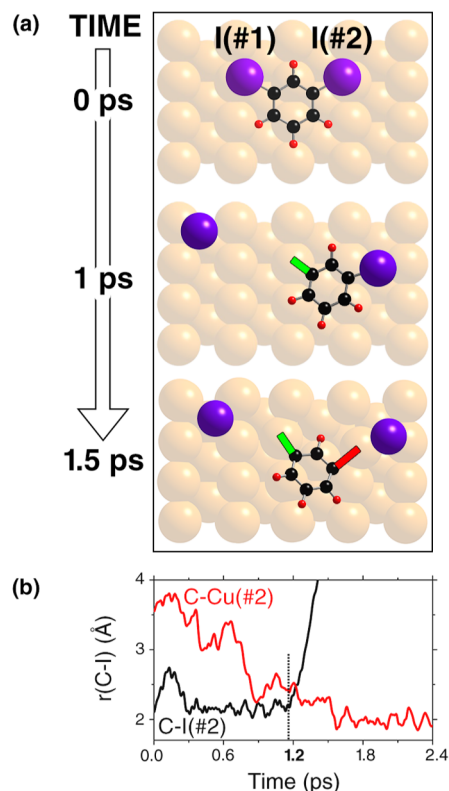


Figure 7. Computed dynamics for the *concerted* pathway. Panel a shows time evolution of the system until both C–I bonds break at 1.5 ps. A half-electron was placed in each of I(#1) and I(#2) for $t^* = 57$ fs. The green line indicates the C–Cu bond which formed first; the red line indicates the C–Cu bond which formed later. Panel b shows internuclear separation of C–I(#2) and C–Cu plotted against time. The onset of C–I(#2) bond breaking and C–Cu bond formation is at 1.2 ps.

two-bond dissociation occurs in a time short compared with molecular rotation. A similar mechanism of *concerted* reaction by single electron impact was reported previously for CH_2I_2 on $\text{Cu}(110)$, in which the I2S model predicted that the first C–I bond would break promptly, and the second ~ 0.5 ps later due to internal excitation of the CH_2I fragment.³⁸

2.5. Time-Resolved Dynamics. The contrasting outcomes as between the *successive* and the *concerted* reaction pathways for electron-induced reaction of mDIB analyzed here with the aid of a theoretical model correlate a long-lived intermediate (IPh) in the first case, *successive*, in contrast to a short-lived intermediate in the second, *concerted*. This suggests the possibility of deliberately limiting the lifetime of an intermediate, and thereby altering the reaction dynamics. This would be achieved by using one electron of a successive pair of electrons to initiate reaction across the surface, and the second electron to terminate the dynamics by a second stage of dissociation. The termination step is well described, for example, in the work of the Bartels group in their study of 2,5-dichlorothiophenol on $\text{Cu}(111)$ at 15 K, in which adsorbate rotation was halted by electron-induced severance of a molecular S–H bond.³⁹ In our proposal, termination of the lifetime of the IPh intermediate is by electron-induced breaking of the C–I bond in IPh (the second bond of mDIB).

For successive two-electron reaction it should frequently be possible to initiate surface motion with a first electron, and terminate it with a second. The reaction dynamics could then be probed by introducing a known time delay, Δt , between the first and second electrons, and subsequently monitoring the reaction-product distribution by STM as a function of Δt . In the *successive* reaction pathway examined in the present work, the first electron forms IPh and the second dissociates the IPh. If the time delay between the two impacting electrons is made shorter than the rotational lifetime of the IPh radical, the first electron will have initiated rotation and the second terminated it. The surface dynamics in the selected time interval would be evident in the product angular distribution of the two chemisorbed I atoms, recorded subsequently by (conventional) STM for a selected Δt .

The time resolution would depend only on that achievable between the pair of electrons or photoelectrons that induce reaction. Time delays measured in femtoseconds are achievable by successive laser pulses, in established “two-pulse correlation” schemes.^{40–42} Since the yield of reaction products per incident electron in the present instance is low, the experiment would require substantial localized electron current. Progress has recently been reported in confining electron dosing to a nanoscale region with femtosecond temporal resolution.⁴³

We have performed a set of calculations to illustrate such an experiment. We used the I2S model to obtain reaction outcomes as a function of the delay Δt between pairs of electrons inducing successive reactions. We considered pathway C to exemplify the method (experiment would show, in addition, examples of products from paths A and B). Figure 8 shows the final state product distributions at successive Δt for path C. The first electron breaks the C–I bond (#1) of mDIB, and the second breaks the C–I bond (#2) of the product of first-bond breaking, following a delay Δt . The values used for Δt were 0.3, 0.6, 2.0, and 3.4 ps (using for each case the minimum t^* that gave reaction). The differing final positions of the I atom(#2) as a function of Δt are a result of the different extents of rotation of the IPh in the differing time intervals,

COMPUTED DYNAMICS AS A FUNCTION OF TIME-DELAY, Δt

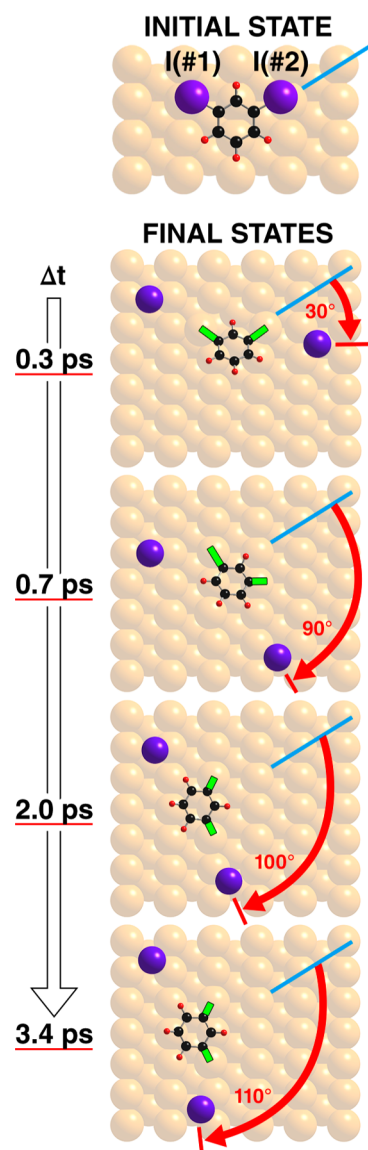


Figure 8. Computed dynamics in trajectory C of the successive pathway for two-bond breaking, one C–I bond for each of two successive electrons at varied time delay, Δt . The breaking of C–I(#2) at $\Delta t = 0.3, 0.7, 1.3, 2.0,$ and 3.4 ps was computed by placing the second electron on I(#2) for a minimum t^* required for bond breaking. The heavy green line indicates the C–Cu bond. The blue line indicates the initial C–I(#2) bond direction, while the short red line shows the direction of the axis linking the chemisorbed I(#2) to the central Ph'.

illustrative of time-resolved dynamics without need of time-resolved imaging.

3. CONCLUSIONS

Scanning Tunneling Microscopy (STM) was used to examine the physisorption and then the electron-induced reaction of meta-diiodobenzene (mDIB) on $\text{Cu}(110)$ at 4.6 K. Electron-induced reaction of the major physisorbed state, “Row”, with its C_2 symmetry axis along the Cu row was shown to proceed by two pathways, exhibiting contrasting dynamics. In the major *successive* reaction, the impact of a first incident electron was

found to break one C–I bond of the physisorbed mDIB reagent, leading to three distinct product alignments, which were confirmed by the observation of three distinct angular distributions for the second I atom coming from the breaking of the second C–I bond. These experimental findings strongly suggested that the iodophenyl product had rotated in-plane directly following first-bond breaking. By contrast, in the minor *concerted* pathway, the impact of a single incident electron was found to break both C–I bonds of the physisorbed mDIB reagent, leading to the observation of a pair of I atoms recoiling from an unrotated mDIB molecule.

Both pathways, *successive* and *concerted*, were simulated by the Impulsive Two-State (I2S) model implemented in DFT. In the major *successive* pathway, single electrons gave single C–I bond breaking, whereas in the minor *concerted* pathway, a single electron broke both C–I bonds. In the *successive* pathway, the time interval between bond-breaking events permitted substantial in-plane rotation of the IPh intermediate under the influence of C–Cu bond formation. In the *concerted* pathway, however, single-electron breaking of both C–I bonds was computed to occur in a time too short for IPh rotation. This analysis suggested a means of obtaining time-resolved reaction dynamics (without time-resolved STM) by varying the delay between electrons responsible for initiating and terminating motion across a surface. A computed example of time-resolved dynamics obtained by this novel means is presented.

The product rotation observed here is of interest not only as a possible “clock” against which to time reaction dynamics but also as a means to propulsion in molecular motors.¹ In this latter context it is noteworthy that the system examined here leads to largely unidirectional product rotation, favorable therefore to the construction of molecular motors. In work on related systems, under way, we examine the sources of such directional rotation.

■ ASSOCIATED CONTENT

Supporting Information

The Supporting Information is available free of charge on the ACS Publications website at DOI: 10.1021/jacs.6b03101.

Materials and methods, additional experimental details, single-molecule reaction rate analysis for competing pathways, additional ab-initio calculation results (PDF)

■ AUTHOR INFORMATION

Corresponding Author

*jpolanyi@chem.utoronto.ca

Present Address

[‡]National University of Singapore, Center for Advanced 2D Materials, 1 CREATE Way, CREATE Tower, Singapore, 138602.

Author Contributions

[†]K.A., K.H., and L.L. contributed equally to this work.

Notes

The authors declare no competing financial interest.

■ ACKNOWLEDGMENTS

We thank Oliver MacLean for helpful discussions and Zhanyu Ning, Chen-Guang Wang, and Zhixin Hu for assistance in the DFT calculations. This work was funded by the Natural Sciences and Engineering Research Council of Canada

(NSERC) and the University of Toronto NSERC General Research Fund. K.A. thanks the Connaught International Scholarship for Doctoral Students for financial support. Computations were performed on the Tightly Coupled System (TCS) at SciNet HPC Consortium. SciNet is funded by the Canada Foundation for Innovation under the auspices of Compute Canada, the Government of Ontario, Ontario Research Fund—Research Excellence, and the University of Toronto.

■ REFERENCES

- (1) De Feyter, S. *Nat. Nanotechnol.* **2011**, *6*, 610–611.
- (2) Murphy, C. J.; Sykes, E. C. H. *Chem. Rec.* **2014**, *14*, 834–840.
- (3) Stipe, B. C.; Rezaei, M. A.; Ho, W.; Gao, S.; Persson, M.; Lundqvist, B. I. *Phys. Rev. Lett.* **1997**, *78*, 4410–4413.
- (4) Stipe, B. C.; Rezaei, M. A.; Ho, W. *Science* **1998**, *279*, 1907–1909.
- (5) Tierney, H. L.; Murphy, C. J.; Jewell, A. D.; Baber, A. E.; Iski, E. V.; Khodaverdian, H. Y.; McGuire, A. F.; Klebanov, N.; Sykes, E. C. H. *Nat. Nanotechnol.* **2011**, *6*, 625–629.
- (6) Kim, H. W.; Han, M.; Shin, H.-J.; Lim, S.; Oh, Y.; Tamada, K.; Hara, M.; Kim, Y.; Kawai, M.; Kuk, Y. *Phys. Rev. Lett.* **2011**, *106*, 146101.
- (7) Avouris, P.; Wolkow, R. *Phys. Rev. B: Condens. Matter Mater. Phys.* **1989**, *39*, 5091–5100.
- (8) Dujardin, G.; Walkup, R. E.; Avouris, P. H. *Science* **1992**, *255*, 1232–1235.
- (9) Bartels, L.; Meyer, G.; Rieder, K.-H.; Velic, D.; Knoesel, E.; Hotzel, A.; Wolf, M.; Ertl, G. *Phys. Rev. Lett.* **1998**, *80*, 2004–2007.
- (10) Ho, W. *J. Chem. Phys.* **2002**, *117*, 11033.
- (11) Komeda, T.; Kim, Y.; Fujita, Y.; Sainoo, Y.; Kawai, M. *J. Chem. Phys.* **2004**, *120*, 5347–5352.
- (12) Morgenstern, K. *Acc. Chem. Res.* **2009**, *42*, 213–223.
- (13) Shin, H.-J.; Jung, J.; Motobayashi, K.; Yanagisawa, S.; Morikawa, Y.; Kim, Y.; Kawai, M. *Nat. Mater.* **2010**, *9*, 442–447.
- (14) Ullmann, F. *Justus Liebigs Ann. Chem.* **1904**, *332*, 38–81.
- (15) Hla, S. W.; Bartels, L.; Meyer, G.; Rieder, K.-H. *Phys. Rev. Lett.* **2000**, *85*, 2777–2780.
- (16) McCarty, G. S.; Weiss, P. S. *J. Phys. Chem. B* **2002**, *106*, 8005–8008.
- (17) Sloan, P. A.; Palmer, R. E. *Nature* **2005**, *434*, 367–371.
- (18) Sakulsermsuk, S.; Sloan, P. A.; Palmer, R. E. *ACS Nano* **2010**, *4*, 7344–7348.
- (19) Lewis, E. A.; Murphy, C. J.; Liriano, M. L.; Sykes, E. C. H. *Chem. Commun.* **2014**, *50*, 1006–1008.
- (20) McCarty, G. S.; Weiss, P. S. *J. Am. Chem. Soc.* **2004**, *126*, 16772–16776.
- (21) Lipton-Duffin, J. A.; Ivasenko, O.; Perepichka, D. F.; Rosei, F. *Small* **2009**, *5*, 592–597.
- (22) Lahrood, A. R.; Bjork, J.; Heckl, W. M.; Lackinger, M. *Chem. Commun.* **2015**, *51*, 13301–13304.
- (23) Leung, L.; Lim, T.; Ning, Z.; Polanyi, J. C. *J. Am. Chem. Soc.* **2012**, *134*, 9320–9326.
- (24) Huang, K.; Leung, L.; Lim, T.; Ning, Z.; Polanyi, J. C. *J. Am. Chem. Soc.* **2013**, *135*, 6220–6225.
- (25) Eisenstein, A.; Leung, L.; Lim, T.; Ning, Z.; Polanyi, J. C. *Faraday Discuss.* **2012**, *157*, 337–353.
- (26) Leung, L.; Lim, T.; Ning, Z.; Polanyi, J. C.; Ji, W.; Wang, C.-G. *J. Phys. Chem. C* **2015**, *119*, 26038–26045.
- (27) Huang, K.; Leung, L.; Lim, T.; Ning, Z.; Polanyi, J. C. *ACS Nano* **2014**, *8*, 12468–12475.
- (28) Panosetti, C.; Hofer, W. A. *J. Comput. Chem.* **2012**, *33*, 1623–1631.
- (29) Menzel, D.; Gomer, R. *J. Chem. Phys.* **1964**, *41*, 3311–3328.
- (30) Redhead, P. A. *Can. J. Phys.* **1964**, *42*, 886–905.
- (31) Henkelman, G.; Uberuaga, B. P.; Jónsson, H. *J. Chem. Phys.* **2000**, *113*, 9901–9904.
- (32) Dougherty, D. B.; Lee, J.; Yates, J. T. *J. Phys. Chem. B* **2006**, *110*, 20077–20080.

- (33) Riedel, D. *J. Phys.: Condens. Matter* **2010**, *22*, 264009.
- (34) Leung, L.; Lim, T.; Polanyi, J. C.; Hofer, W. A. *Nano Lett.* **2011**, *11*, 4113–4117.
- (35) Huang, K.; MacLean, O.; Guo, S. Y.; McNab, I. R.; Ning, Z.; Wang, C.-G.; Ji, W.; Polanyi, J. C. *Surf. Sci.* **2016**, DOI: [10.1016/j.susc.2016.02.001](https://doi.org/10.1016/j.susc.2016.02.001).
- (36) Velic, D.; Hotzel, A.; Wolf, M.; Ertl, G. *J. Chem. Phys.* **1998**, *109*, 9155–9165.
- (37) Gadzuk, J. W. *Phys. Rev. B: Condens. Matter Mater. Phys.* **1991**, *44*, 13466–13477.
- (38) Chatterjee, A.; Cheng, F.; Leung, L.; Luo, M.; Ning, Z.; Polanyi, J. C. *J. Phys. Chem. C* **2014**, *118*, 25525–25533.
- (39) Rao, B. V.; Kwon, K.-Y.; Liu, A.; Bartels, L. *J. Chem. Phys.* **2003**, *119*, 10879–10884.
- (40) Budde, F.; Heinz, T. F.; Loy, M. M. T.; Misewich, J. A.; de Rougemont, F.; Zacharias, H. *Phys. Rev. Lett.* **1991**, *66*, 3024–3027.
- (41) Busch, D. G.; Gao, S.; Pelak, R. A.; Booth, M. F.; Ho, W. *Phys. Rev. Lett.* **1995**, *75*, 673–676.
- (42) Gao, S.; Busch, D. G.; Ho, W. *Surf. Sci.* **1995**, *344*, L1252–L1258.
- (43) Müller, M.; Kravtsov, V.; Paarmann, A.; Raschke, M. B.; Ernstorfer, R. *ACS Photonics* **2016**, *3*, 611–619.